

Supplement of Atmos. Chem. Phys., 14, 10085–10102, 2014
<http://www.atmos-chem-phys.net/14/10085/2014/>
doi:10.5194/acp-14-10085-2014-supplement
© Author(s) 2014. CC Attribution 3.0 License.



Supplement of

Concentrations and fluxes of isoprene and oxygenated VOCs at a French Mediterranean oak forest

C. Kalogridis et al.

Correspondence to: V. Gros (valerie.gros@lsce.ipsl.fr)

1. Calibration and volume mixing ratios (VMR) calculations

Calibration coefficients, also called normalized sensitivities (S_{norm}) were calculated for each atomic mass unit (amu, m/z) using the approach of Taipale et al., (2008). Normalized sensitivities S_{norm} were expressed in units of normalized counts/sec/ppbv (ncps/ppbv) as follows:

$$S_{norm} = \frac{I(RH_i^+)_{norm}}{VMR_{standar}}, \quad (S1)$$

$$I(RH_i^+)_{norm} = 10^6 \times \left(\frac{I(RH_i^+)}{m/z_{21} * 500 + m/z_{37}} - \frac{I(RH_i^+)_{zero}}{m/z_{21_{zero}} * 500 + m/z_{37_{zero}}} \right), \quad (S2)$$

where, $I(RH_i^+)$ is the ion count signal at mass m/z_i (units:cps), $I(RH_i^+)_{zero}$ is the ion count signal at mass m/z_i from the zero air (cps), m/z 21 and m/z 37 the counts of the primary ($H_3^{18}O^+$) and reagent clusters ($H_3^{16}O^+ H_2^{16}O^+$) (cps), m/z 21_{zero} and m/z 37_{zero} the counts of the primary and reagent clusters when measuring from the zero air (cps), $I(RH_i^+)_{norm}$ the normalized ion count rate of $I(RH^+)$ (ncps) and VMR the volume mixing ratios (ppbv).

2. PTR-MS based water vapour flux measurements and comparison with a reference system.

Water vapour concentrations and fluxes were measured using a standard reference system based on the combination of a closed path infrared gas analyzer (IRGA, Model 7000, LiCOR) and the sonic anemometer. Both instruments were set to a sampling frequency of 20 Hz. Ambient air close to the sonic sensor head was continuously sampled through the main line (inlet at 10 m) leading to the IRGA instrument. Fluxes were calculated by the eddy covariance (EC) method, as implemented before by Loubet et al., (2011). Additionally a high frequency losses corrections was implemented based on the co-give method as in (Ammann et al., 2006)

EC water vapour fluxes from the standard reference system were also compared to DEC water vapour fluxes derived from the signal at m/z 37 of the PTR-MS (Ammann et al., 2006). The same anemometer was used for the DEC flux measurements with the PTR-MS as for the IRGA system.

In the PTR-MS, water vapour was detected at m/z 37, a mass corresponding to the cluster ion $\text{H}_3\text{O}^+ \text{H}_2\text{O}^+$ present in the drift tube. Water clusters in the drift tube originate from the ion source but also from the water vapour in the sample air. It is expected that the contribution of the ion source to the m/z 37 is relatively constant and thus, there is a quantitative relationship between the signal at m/z 37 and the concentration of the water vapour (Ammann et al., 2006). Ion counts at m/z 37 were calibrated against the reference IRGA concentration, in order to investigate the relationship between the m/z 37 signal and the water vapour concentration in the sampled air (Fig. S1).

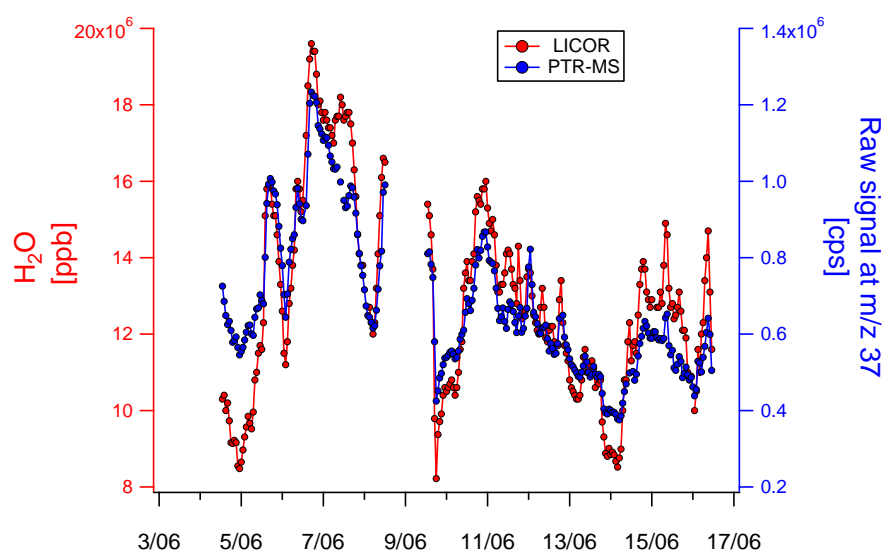


Figure S1. Time series of the PTR-MS m/z 37 signal (units: cps) and of water vapour as measured by the closed path infrared gas analyser IRGA.

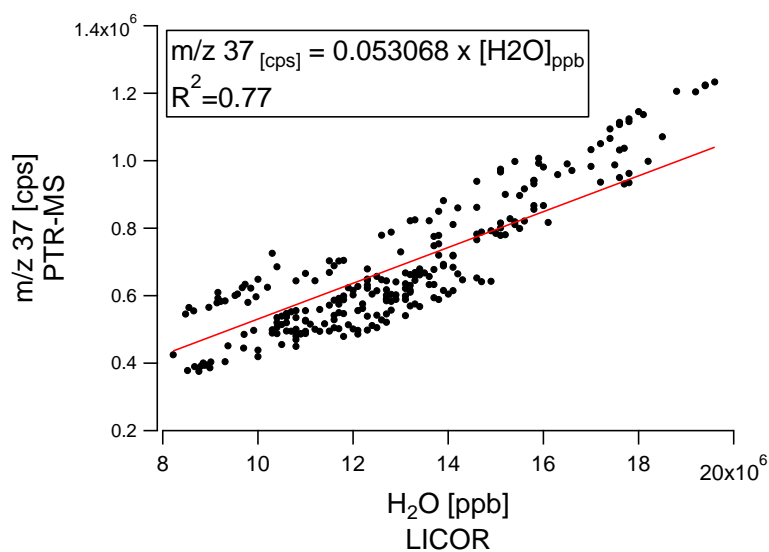


Figure S2. Relationship between the PTR-MS m/z 37 signal (units: cps) and the water vapour concentration (units: ppb) as measured by the closed path infrared gas analyser IRGA.

The raw signal at m/z 37 showed a linear relationship to the IRGA water vapour concentration with a coefficient of determination, R^2 , of 0.77. The following equation was used for the calibration of water vapour concentration against the m/z 37 signal:

$$[H_2O]_{ppb} = m/z\ 37_{cps} \times \frac{1}{0.053} \quad (S5)$$

After calibration, m/z 37 fluxes were calculated in $g.m^{-2}.s^{-1}$ with the same LabVIEW algorithm used for the other VOC fluxes and then converted in latent heat fluxes LE (units: $W.m^{-2}$) using the latent heat of evaporation constant ($Lv = 2400\ J\ g^{-1}$ at $25^\circ C$):

$$LE_{W.m^{-2}} = LE_{J\ s^{-1}\ m^{-2}} = F(water)_{g\ m^{-2}\ s^{-1}} \times Lv_{J\ g^{-1}} \quad (S6)$$

The resulting calibrated PTR-MS based latent heat fluxes are plotted along the IRGA fluxes in Fig S3.

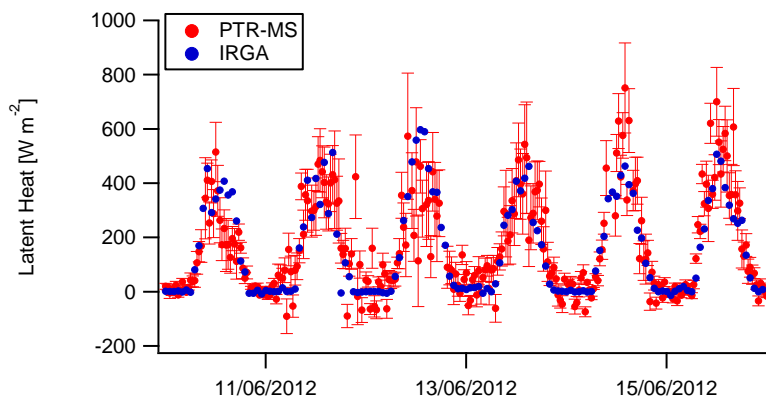


Figure S3. Time series of the PTR-MS based and IRGA latent heat fluxes

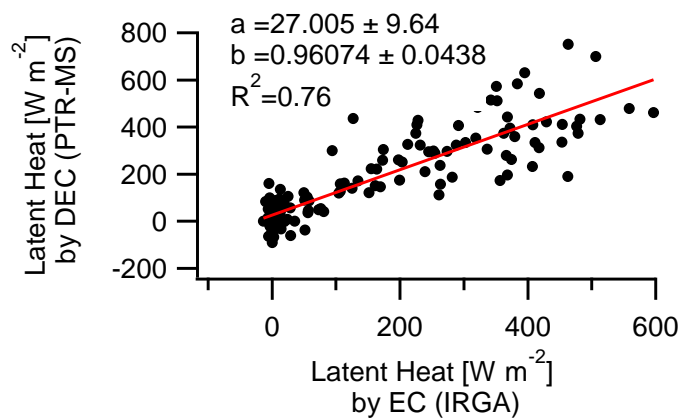


Figure S4. Relationship between the latent heat as measured by the PTR-MS and the closed path infrared gas analyser IRGA.

Water vapour fluxes obtained with the PTR-MS were highly comparable to the results of the IRGA reference system. A linear relation was found between the latent heat measured by DEC (PTR-MS) and conventional EC (IRGA), with a coefficient of correlation, R^2 , of 0.76. This good agreement supports our PTR-MS eddy flux measurements of VOCs.

3 Comparison between DEC fluxes and vertical concentration gradients

Isoprene fluxes derived by DEC were also compared to the vertical gradient of isoprene concentration inside the canopy multiplied by the friction velocity:

$$u^* \times \frac{\partial C}{\partial z} = u^* \times \frac{c_{iso(2m)} - c_{iso(10m)}}{|z_{2m} - z_{10m}|} \quad (S7)$$

Although one cannot quantitatively derive a flux from the gradient method, because the lower measurement height was not only within the roughness sublayer, but also located below some of the sources inside the canopy, the correlation found was fairly strong ($R^2 = 0.6$), lending further confidence to the DEC flux measurements (Figure S5). Here, the measured gradient stands for a proxy of the above-canopy gradient and u^* as a proxy for the eddy-diffusivity, which in reality depends further on atmospheric stability.

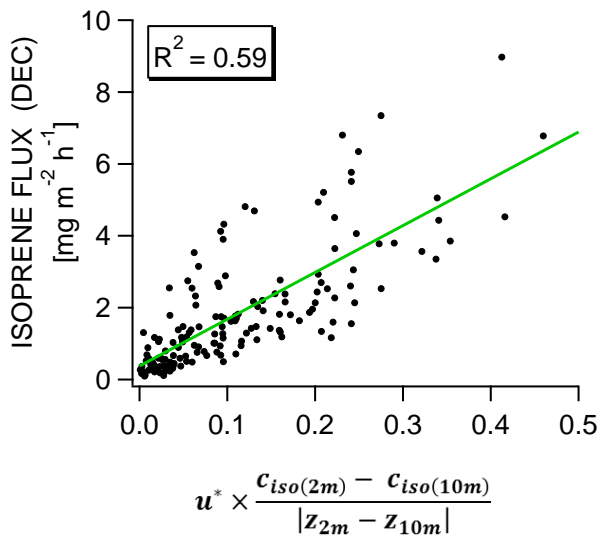


Figure S5. Correlation between isoprene fluxes measured above the canopy by DEC and the gradient of isoprene concentration (between 2 m and 10 m) multiplied by the friction velocity.

4 Time τ for diffusion transport of a trace gas

The turbulent transport time τ between the measurement height (z_{ref}) and the ground surface can be expressed as the transfer resistance through each layer multiplied by the layer height (Garland, 1977).

$$\tau = \tau_{in_canopy} + \tau_{above_canopy} \quad (S8.1)$$

$$= Ra_{canopy} \cdot (d + z_{0(M)}) + Ra_{zref} (z_{ref} - d - z_{0(M)}) \quad (S8.2)$$

where d is the canopy displacement height and z_0 is the canopy roughness length. Estimates from the literature gives $d = 0.7 \cdot h_c$ where h_c is the canopy height, and $z_{0(M)} = 0.13 \cdot h_c$. Turbulent resistances within and above the canopy, Ra_{canopy} and Ra_{zref} respectively, are expressed as:

$$Ra_{canopy} = \frac{h_c \cdot \exp^{\alpha_u}}{\alpha_u \cdot K_m(h_c)} \cdot \left(\exp \frac{-\alpha_u \cdot z_{0(s)}}{h_c} - \exp \frac{-\alpha_u \cdot (d + z_0)}{h_c} \right) \quad (S9.1)$$

$$Ra_{zref} = \frac{1}{k^2 \cdot u(z_{ref})} \cdot \left(\ln \frac{z_{ref} - d}{z_{0(T)}} - \Psi_H \left(\frac{z_{ref} - d}{L} \right) \right) \cdot \left(\ln \frac{z_{ref} - d}{z_{0(M)}} - \Psi_M \left(\frac{z_{ref} - d}{L} \right) \right) \quad (S9.2)$$

where $k(=0.4)$ is the von Kármán constant, $z_{0(M)}$ and $z_{0(T)}$ are the canopy roughness length for temperature and momentum, $z_{0(s)}$ ($=0.02$ m; (Personne et al., 2009)) is the ground surface roughness length below the canopy; α_u is the attenuation coefficient for the decrease of the wind speed inside the canopy, defined as LAI/2 (Yi, 2008), $K_m(h_c)$ is the eddy diffusivity at the canopy height; and Ψ_M and Ψ_H are dimensionless stability correction functions for heat and momentum (Dyer, 1974).

In the current study the transport time was estimated to be in the range of 30-60 s in daytime.

5 GC-MS (cartridges)/PTR-MS monoterpene field comparison

Additionally to the measurements presented in the manuscript, monoterpene samples have been collected inside the forest of the O₃HP, using sampling cartridges containing Tenax TA

absorbent. The same storage procedure and analytical method (GC/MS) than for isoprene cartridges has been applied (see section 2.2 of the manuscript). Over the whole measurement period, α -pinene was representing $80\pm 13\%$ of the total monoterpenes at the site. Limonene was the second most abundant monoterpene ($15\pm 9\%$), but its mixing ratios were very close to the detection limits, and always below 15 ppt Other monoterpenes, such as camphene, have been detected but were usually below the quantification limit.

A comparison between the GC-MS and PTR-MS monoterpenes measurements was conducted at the O₃HP on June 17th, when both PTR-MS and cartridges were sampling at 2 m height, i.e inside the canopy. On the day of the intercomparison, the only monoterpene detected from the cartridge analysis was α -pinene. The PTR-MS and GC-MS monoterpene measurements were in good quantitative agreement, even though a small $\sim 14\%$ positive bias in the PTR-MS measurements has been observed. A correlation plot of the PTR-MS versus GC-MS α pinene measurements was described by a linear regression equation and a $R^2=0.8595$ (Fig. S6).

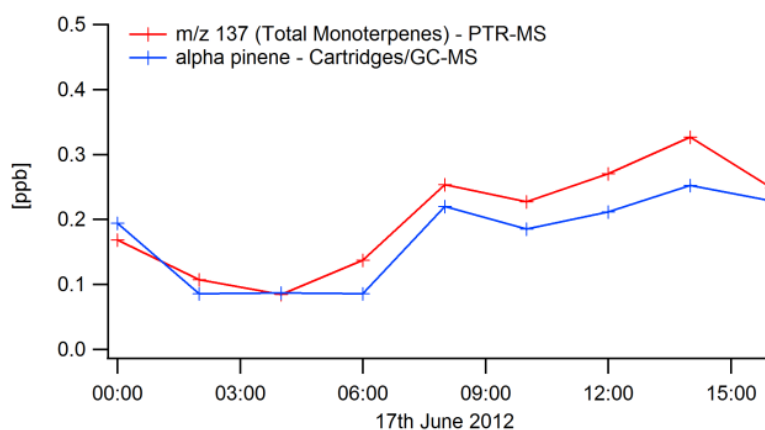


Figure S6 Time series of total monoterpenes and α -pinene as measured by PTR-MS and GC-MS respectively

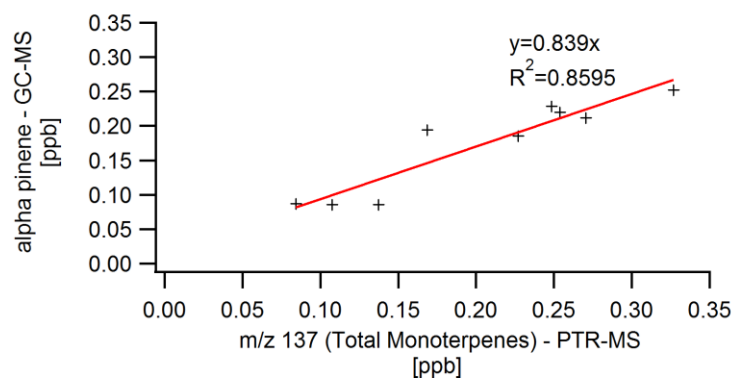


Figure S7. Relationship between the PTR-MS m/z 37 signal (units: cps) and α -pinene concentration (units: ppb) as measured by GC-MS analysis of cartridge samples.

References

- Ammann, C., Brunner, A., Spirig, C., Neftel, A., 2006. Technical note: Water vapour concentration and flux measurements with PTR-MS. *Atmospheric Chemistry and Physics* 6, 4643–4651.
- De Gouw, J., Warneke, C., 2006. Measurements of volatile organic compounds in the earth's atmosphere using proton-transfer-reaction mass spectrometry. *Mass Spectrometry Reviews* 26, 223–257.
- Dyer, A.J., 1974. A review of flux-profile relationships. *Boundary-Layer Meteorol* 7, 363–372.
- Garland, J.A., 1977. The Dry Deposition of Sulphur Dioxide to Land and Water Surfaces. *Proc. R. Soc. Lond. A* 354, 245–268.
- Loubet, B., Laville, P., Lehuger, S., Larmanou, E., Fléchar, C., Mascher, N., Genermont, S., Roche, R., Ferrara, R.M., Stella, P., Personne, E., Durand, B., Decuq, C., Flura, D., Masson, S., Fanucci, O., Rampon, J.-N., Siemens, J., Kindler, R., Gabrielle, B., Schrumpf, M., Cellier, P., 2011. Carbon, nitrogen and Greenhouse gases budgets over a four years crop rotation in northern France. *Plant Soil* 343, 109–137.
- Personne, E., Loubet, B., Herrmann, B., Mattsson, M., Schjoerring, J.K., Nemitz, E., Sutton, M.A., Cellier, P., 2009. SURFATM-NH₃: a model combining the surface energy balance and bi-directional exchanges of ammonia applied at the field scale. *Biogeosciences* 6, 1371–1388.
- Taipale, R., Ruuskanen, T.M., Rinne, J., Kajos, M.K., Hakola, H., Pohja, T., Kulmala, M., 2008. Technical Note: Quantitative long-term measurements of VOC concentrations by PTR-MS – measurement, calibration, and volume mixing ratio calculation methods. *Atmos. Chem. Phys.* 8, 6681–6698.
- Yi, C., 2008. Momentum Transfer within Canopies. *Journal of Applied Meteorology and Climatology* 47, 262–275.
- Zhao, J., Zhang, R., 2004. Proton transfer reaction rate constants between hydronium ion (H₃O⁺) and volatile organic compounds. *Atmospheric Environment* 38, 2177–2185.